JOURNAL OF GEOPHYSICAL RESEARCH, VOL. 106, NO. D4, PAGES 3529–3540, FEBRUARY 27, 2001

Modeling methane fluxes in wetlands with gas-transporting plants
2. Soil layer scale

Reinoud Segers

Group Plant Production Systems, Laboratory of Theoretical Production Ecology, Wageningen University, Wageningen, The Netherlands

Cornelis Rappoldt

Biological Centre, University of Groningen, the Netherlands

Peter A. Leffelaar

Group Plant Production Systems, Laboratory of Theoretical Production Ecology, Wageningen University, Wageningen, The Netherlands

Abstract. Methane dynamics in a water-saturated soil layer with gas-transporting roots is modeled with a weighed set of single-root model systems. Each model system consists of a soil cylinder with a gas-transporting root along its axis or a soil sphere with a gas-transporting root at its center. The weights associated with a different cylinder or sphere radius were deduced from root architecture. Methane dynamics in each single-root model system are calculated using a single-root model from the previous paper. From this full model a simplified model was deduced consisting of an oxygen-saturated and an oxygen-unsaturated model system. An even more simplified model was deduced, called the homogeneous model. In this model the concentrations are homogeneous in the whole soil layer. Simulation results of the simplified model are closer to the simulation results of the full model than the simulation results of the homogeneous model. The overall effect of the simplifications on simulated methane emissions are small, though the underlying processes are affected more severely, depending on simulation time and parameters. At high root densities and at large times, under stationary conditions, root density is proportional to simulated methane fluxes, provided that carbon availability is proportional to root density. Sensitivity analysis shows that lack of knowledge on root gas-transport is an important limitation for the predictability of methane fluxes via the processes at the kinetic level.

1. Introduction

Wetland soils with gas-transporting plants are an important source of methane [*Prather et al.*, 1995; *Nykänen et al.*, 1998; *Bellisario et al.*, 1999]. Variation in methane fluxes from these systems is large and difficult to understand due to the dynamic, nonlinear interactions between underlying processes [*Conrad*, 1993; *Wang*, 1996; *Segers*, 1998]. This paper is the second in a series of three, which aims to unravel these interactions by explicitly relating knowledge at the kinetic level to methane fluxes at the plot level.

In paper 1 [*Segers and Leffelaar*, this issue (a)] the interactions between the kinetic and the diffusion processes around a single gas-transporting root were investigated by developing, simplifying, and testing a reaction-diffusion model. In this paper this model is scaled up from a single root to a soil layer. In paper 3 [*Segers and Leffelaar*, this issue (b)] the step is made to a model for methane fluxes at the plot scale, allowing vertical gradients and, temporarily, water unsaturation. At the (discretized) soil layer scale, studied in this paper, it is assumed that root density, water content, and temperature are constant. Furthermore, in this paper, only water-saturated soil is considered in which gas exchange with the atmosphere occurs via the plant roots and ebullition. Hence, the focus is on the role of a system of gas-transporting roots in methane dynamics.

Paper number 2000JD900483.
0148-0227/01/2000JD900483$09.00

2. Model Description

2.1. A Single-Root Model System

The starting point of the analysis is a single-root model system [*Segers and Leffelaar*, this issue (a)]. The soil is represented by a hollow infinite cylinder or a hollow sphere. The inner surface represents the root surface via which gas exchange with the atmosphere is possible. The outer surface, at distance R from the center, is half the distance to the next root at which fluxes are zero. Within this system, methane, oxygen, carbon dioxide, molecular nitrogen, and an arbitrary alternative terminal electron acceptor in reduced and oxidized form react and diffuse. These processes cause the oxygen concentration to decrease with distance from the root. Near the root, aerobic processes occur: aerobic respiration, methane oxidation, and electron acceptor reoxidation. Far from the root, anaerobic processes occur: methane production and

electron acceptor reduction. The system as a whole imports oxygen and exports methane via the root. Both a cylindrical and a spherical geometry are studied. The cylindrical geometry represents a situation where the whole root is active, while the spherical geometry represents a situation where only the root tip is active. In paper 1 [*Segers and Leffelaar*, this issue (a)] reaction-diffusion equations for the six compounds were numerically solved to study the behavior of this system. Using insight in the order of magnitude of parameters, this full single-root model was simplified by a quasi-steady-state assumption for oxygen and by spatially averaging the equations for the other compounds. The resulting simplified single-root model produced almost the same results as the full model and is therefore used in this paper. The derivation of this simplified model in the work of *Segers and Leffelaar* [this issue (a)] is rather long. Therefore a shorter description of this simplified model is added (Appendix A) to make this paper easier to read.

2.2. A Soil Layer With a Root System: a Weighted Set of Single-Root Systems With Different Radii

The interaction between diffusion and reactions is mainly determined by surface-area-to-volumeratios and not by the exact geometry [*Bird et al.*, 1960]. The surface-area-to-volumeratio is closely related to the distance of a point in soil to gas exchanging surface. Using this insight, *Rappoldt* [1990, 1992] developed an algorithm to represent the geometry of a complex medium by a weighed set of simple geometric forms. The basic idea (Figure 1) is that the probability density distribution (PDF) of the distance to the nearest gas-exchanging surface of the model system is matched to the distance PDF of the real system. The weights needed to achieve this are a representation of the geometry.

Here a rooted soil layer is represented by a weighed set of either cylindrical or spherical single-root model systems with variable radii R. Weights $v(R)$ are used to calculate soil layer-averaged properties for each quantity χ, which can be defined in a point.

$$\bar{\bar{\chi}}(t) = \int_0^\infty v(R)\, \bar{\chi}(R,t)\, dR. \tag{1}$$

The notation section lists the symbols. For example, χ is the methane concentration, or the volumetric rate of electron acceptor reoxidation. The dynamics of each $\bar{\chi}$ is calculated with the simplified model from paper 1 (*Segers and Leffelaar* [this issue (a)] and Appendix A). Weights $v(R)$ are derived from the PDF of the distance to the nearest root, $g(x)$ (*Rappoldt* [1992] and Appendix B),

$$v_c(R) = \frac{1}{2}\, g(x) - \frac{1}{2}\, x\, \frac{dg(x)}{dx}\Big|_{x=R}, \tag{2a}$$

$$v_s(R) = \frac{2}{3}\, g(x) - \frac{1}{3}\, x\, \frac{dg(x)}{dx}\Big|_{x=R}; \tag{2b}$$

$g(x)$ can be derived in three ways [*Rappoldt*, 1990, 1992]. Firstly, it can be deduced experimentally from two-dimensional or three-dimensional images of rooted soils. Secondly, it can be calculated numerically from any simulated root system, and thirdly, it can be calculated analytically from simple model root systems with a simple mathematical description. In this paper we took the last two approaches, as these allow us to study the role of the root architecture in methane fluxes. The numerical procedure to deduce $g(x)$ and $v(R)$ from the root system characterized by the parameters c_{rt}, f_{prim}, SRL_{prim}, l_{lat}, and Δx_{lat} is given in Appendix C. To interpret the resulting $g(x)$, also analytical expressions for randomly distributed roots are used (*Ogston* [1958]: 3-D analog of 2-D derivation of *Pielou* [1977, p. 148]).

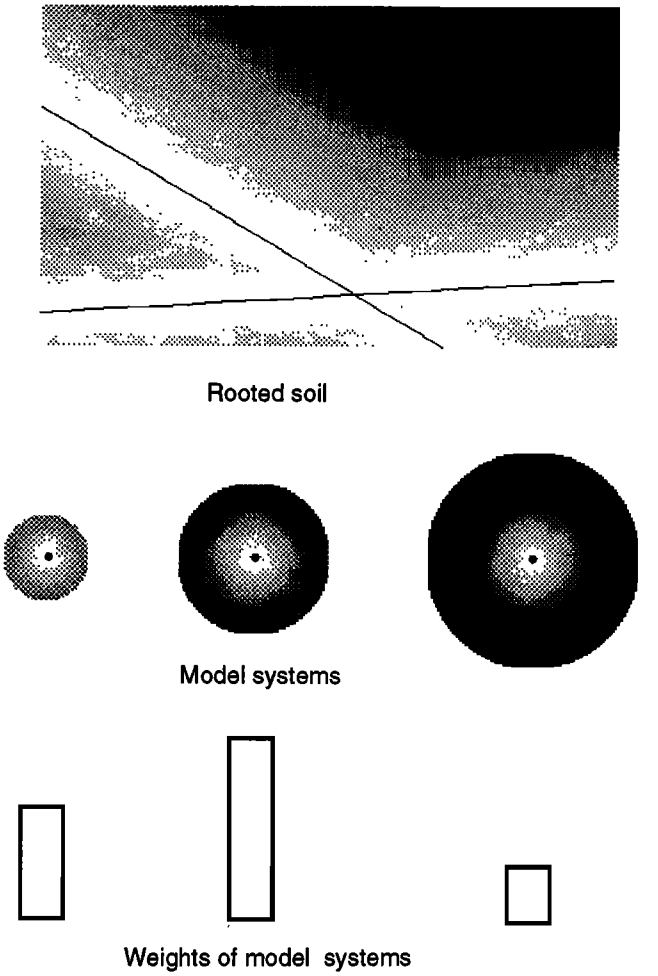

Figure 1. Two-dimensional sketch of the geometry transformation. The rectangle above represents a part of the soil aerated by two arbitrarily arranged roots. The grey value represents the distance to the nearest root: the darker, the larger the distance to the nearest root. The three disks represent model systems with a simple geometry. In the center of these disks there is a root. The model systems are weighed in such a way that the distribution of distances to the nearest root (grey values) in the model systems is equal to the distribution of the distances in the original soil.

$$g_c(x) = 2\,\pi\, L_{tot}\, x\, \exp(-\pi\, L_{tot}\, x^2), \tag{3a}$$

$$g_s(x) = 4\,\pi\, N_{tot}\, x^2 \exp(-\frac{4}{3}\,\pi\, N_{tot}\, x^3), \tag{3b}$$

with corresponding probability density functions (with equations (2))

$$v_c(R) = 2\,\pi^2\, L_{tot}^2\, R^3 \exp(-\pi\, L_{tot}\, R^2), \tag{4a}$$

$$v_s(R) = \frac{16}{3}\,\pi^2\, N_{tot}^2\, R^5 \exp(-\frac{4}{3}\,\pi\, N_{tot}\, R^3). \tag{4b}$$

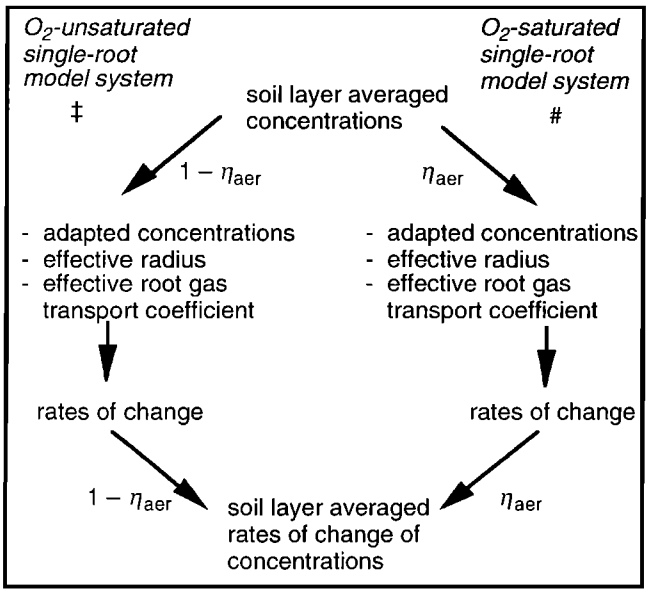

Figure 2. Illustration of calculations for the simplified single-root model.

2.3. Simplified Soil Layer Model

In analogy to the single-root level, a simplified model is formulated at the soil layer level by aggregating over the single-root model systems, to arrive at state variables, concentrations $\bar{\bar{c}}$, at the soil layer level (Figure 2). Each concentration $\bar{\bar{c}}_l$ changes as a result of ebullition $\bar{\bar{b}}_l$, kinetics $\bar{\bar{s}}_l$, and plant mediated transport $\bar{\bar{q}}_l$.

$$\frac{d\bar{\bar{c}}_l}{dt} = \bar{\bar{b}}_l(\bar{\bar{c}}) + \bar{\bar{s}}_l(\bar{\bar{c}}) + \bar{\bar{q}}_l(\bar{\bar{c}}). \tag{5}$$

The starting point of the simplifications are the oxygen dynamics, a key factor. First, the distance to the root at which the soil is aerated is estimated from some dimensionless numbers consisting of ratios between kinetic and transport parameters [*Segers and Leffelaar*, this issue (a), equations (44)-(48)]:

$$R_{aer,0,c} = \sqrt{2\,\beta_0\,(1-c')}\,r_{rt} \tag{6a}$$

$$R_{aer,0,s} = \sqrt[3]{3\,\beta_0\,(1-c')}\,r_{rt} \tag{6b}$$

where β_0 is β with $\omega = 1$. Subsequently, the single-root model systems are divided into two fractions: (1) oxygen-saturated single-root model systems with $R < R_{aer,0}$, with symbol "#" and fraction η_{aer} and (2) oxygen-unsaturated single-root model systems with $R > R_{aer,0}$, with symbol "‡" and fraction $(1 - \eta_{aer})$. Weight function $v(R)$ is used to calculate η_{aer}:

$$\eta_{aer} = \int_0^{R_{aer,0}} v(R)\,dR \tag{7}$$

From the state variables at the soil layer level (concentrations $\bar{\bar{c}}$) the concentrations of oxidized and reduced electron acceptors and methane in the two soil fractions are deduced (Figure 2). This is done by allocating the reduced compounds (reduced electron acceptors and methane) to the oxygen-unsaturated fraction, under the constraint that the concentration of reduced electron acceptors is not higher than the concentration of the total electron acceptor pool (equations (8)-(11)).

$$c_{er}^{\ddagger} = \mathrm{MIN}\left(\frac{\bar{\bar{c}}_{er}}{1-\eta_{aer}}, c_{e_{tot}}\right) \qquad c_{er}^{\#} = \frac{\bar{\bar{c}}_{er} - (1-\eta_{aer})\,c_{er}^{\ddagger}}{\eta_{aer}}, \tag{8}$$

$$c_{eo}^{\ddagger} = c_{e_{tot}} - c_{er}^{\ddagger} \qquad c_{eo}^{\#} = c_{e_{tot}} - c_{er}^{\#}, \tag{9}$$

$$c_{CH_4}^{\ddagger} = \frac{\bar{\bar{c}}_{CH_4}}{(1-\eta_{aer})} \qquad c_{CH_4}^{\#} = 0, \tag{10}$$

$$c_i^{\ddagger} = c_i^{\#} = \bar{\bar{c}}_i \qquad \text{for } i = N_2, CO_2. \tag{11}$$

Now the fractions are considered as two single-root model systems with concentrations $\boldsymbol{c}^{\ddagger}$ and $\boldsymbol{c}^{\#}$ and weights $(1 - \eta_{aer})$ and η_{aer}. Using this, ebullition is calculated with the simplified single-root model (equation (A26)) for each gas i:

$$\bar{\bar{b}}_i = \eta_{aer}\,\bar{b}_i(\boldsymbol{c}^{\#}) + (1-\eta_{aer})\,\bar{b}_i(\boldsymbol{c}^{\ddagger}). \tag{12}$$

For the kinetic rates $\bar{\bar{s}}_i$ the situation is a bit more complicated, because an effective R is needed. An estimate for $\bar{\bar{s}}_i$ is deduced starting from the full soil layer model (equation 1):

$$\bar{\bar{s}}_i = \int_0^{R_{aer,0}} v(R)\,\bar{s}_i(R,\bar{\boldsymbol{c}}(R))\,dR + \int_{R_{aer,0}}^{\infty} v(R)\,\bar{s}_i(R,\bar{\boldsymbol{c}}(R))\,dR. \tag{13}$$

Here the first term represents the kinetics in the oxygen-saturated fraction and the second term represent the kinetics in the oxygen-unsaturated fraction. To resolve the integrals, the dependence of $\bar{s}_i$ on R has to be eliminated. This is done by introducing effective values for R and $\bar{\boldsymbol{c}}$ in the oxygen-saturated and in the oxygen-unsaturated zone:

$$\begin{aligned}\bar{\bar{s}}_i &= \int_0^{R_{aer,0}} v(R)\,\bar{s}_i(R^{\#},\boldsymbol{c}^{\#})\,dR + \int_{R_{aer,0}}^{\infty} v(R)\bar{s}_i(R^{\ddagger},\boldsymbol{c}^{\ddagger})\,dR \\ &= \eta_{aer}\,\bar{s}_i(R^{\#},\boldsymbol{c}^{\#}) + (1-\eta_{aer})\,\bar{s}_i(R^{\ddagger},\boldsymbol{c}^{\ddagger})\end{aligned} \tag{14}$$

Expressions for $\boldsymbol{c}^{\#}$ and $\boldsymbol{c}^{\ddagger}$ are in equations (8)-(11). Effective values for R are estimated in such a way that relative aeration κ, a crucial quantity [*Segers and Leffelaar*, this issue (a)], is calculated as exactly as possible; κ is proportional to $1/R^2$ for the cylindrical case and to $1/R^3$ for the spherical case. Therefore average values of $1/R^2$ and $1/R^3$ are used to calculate effective values of $R_c^{\#}$, $R_c^{\ddagger}$, $R_s^{\#}$, and $R_s^{\ddagger}$. For example,

$$R_c^{\#} = \frac{1}{\sqrt{\dfrac{1}{\eta_{aer}}\displaystyle\int_0^{R_{aer,0}} v(R)\,\frac{1}{R^2}\,dR}}. \tag{15}$$

As root gas-transport does not scale with R in the same way as aeration (equation (A24)), it is calculated with effective gas-transport coefficients, $r_{q,c}^{\#}$, $r_{q,c}^{\ddagger}$, $r_{q,s}^{\#}$, and $r_{q,s}^{\ddagger}$:

$$\bar{\bar{q}} = \eta_{aer}\,\bar{q}(r_q^{\#},\boldsymbol{c}^{\#}) + (1-\eta_{aer})\,\bar{q}(r_q^{\ddagger},\boldsymbol{c}^{\ddagger}). \tag{16}$$

The effective gas-transport coefficients $r_q^{\#}$ and $r_q^{\ddagger}$ are calculated by averaging over the model systems over which they prevail. For example,

$$r_{q,c}^{\ddagger} = \frac{1}{1-\eta_{aer}}\int_{R_{aer,0}}^{\infty} v_c(R)\,r_{q,c}(R)\,dR \tag{17}$$

2.4. Homogeneous Soil Layer Model

In the simplified soil layer model, the soil is represented by an oxygen-saturated and oxygen-unsaturated single-root model system. To investigate the meaning of this distinction, an even more simple soil layer model was tested: the homogeneous soil layer model (equation (18)). In this model, kinetic knowledge [*Segers and Leffelaar*, this issue (a), equations (10)-(33)] is directly applied at the soil layer level to calculate $\bar{\bar{s}}_i(\bar{\bar{c}})$, as *Arah and Stephen* [1998], implying that O_2 is treated like the other gases.

$$\frac{d\bar{\bar{c}}_i}{dt} = \bar{\bar{s}}_i(\bar{\bar{c}}) + \bar{\bar{q}}_i(\bar{\bar{c}}) + \bar{\bar{b}}_i(\bar{\bar{c}}) \quad i = CH_4, O_2, N_2, CO_2, eo, er. \qquad (18)$$

Vegetation-mediated transport $\bar{\bar{q}}_i(\bar{\bar{c}})$ is calculated with a first-order coefficient, $\bar{\bar{r}}_q$, which is calculated from the single-root gas transport coefficients with equation (1). In this coefficient, transport resistance between soil and rhizosphere is incorporated. Bubble formation and transport ($\bar{\bar{b}}_i(\bar{\bar{c}})$) is calculated from equations (A25) and (A26) with the soil-layer-averaged gas concentrations.

2.5. Parameters and Initial Values

To understand methane fluxes in peat soils, it is particularly important to quantify the flows of reactive carbon, and not the total carbon pool, which is very stable in peat [e.g., *Clymo*, 1984; *Bridgham et al.*, 1998]. To do so, the flow of carbon is related to the source, decaying plant material. Here only roots are considered, firstly because the root-shoot ratio of sedges can be much larger than 1 (^{14}C experiments [*Wallén*, 1986; *Saarinen*, 1996]) and, secondly, because this paper focuses on roots. Reference C-mineralization was estimated in such a way that total C-mineralization under complete anaerobiosis is equal to total root turnover:

$$s_{rcm}(T) = Q_{10}^{\frac{T-T_{ref}}{10}} \frac{f_C}{M_C} \frac{c_{rt}}{\tau_{rt}} \frac{1}{f_{an}}. \qquad (19)$$

This approach also covers the incorporation of decaying roots in soil organic matter and the related long term soil organic matter mineralization. Turnover time of roots τ_{rt} of vascular wetland plants is probably between 1 and 10 years for northern wetland sites [*Shaver and Billings*, 1975; *Saarinen*, 1996]. Here τ_{rt} is set at 2 years at the reference temperature (9°C), which is the average temperature in the region of the model application (the Netherlands) [*Segers and Leffelaar*, this issue (b)]. Root exudation was neglected as reliable data for natural wetland plants are absent. If it is important, then here at the soil layer scale, it would imply a higher C-availability per root dw, which can be described with a lower τ_{rt}. This would mean a shift in the range of tested dimensionless parameters, and because we tested a large range, the risk of different conclusions is small.

The model is run with a temperature of 15°C, a typical soil temperature in summer. As in the previous paper [*Segers and Leffelaar*, this issue (a)], all biological processes are temperature dependent with a Q_{10} of 2; f_C was 0.4. Apart from R and s_{rcm}, all other initial conditions and parameters in each single-root model system are the same as in the paper that describes the single root scale [*Segers and Leffelaar*, this issue (a)].

2.6. Numerical Procedures

The weight function $v(R)$ is approximated by N weights w_m in equal distance classes, using a discretized version of equation (2a) [*Rappoldt*, 1992] and equation (2b) (Appendix B). R goes to infinity in case the analytical expressions (equation (4)) are used. Therefore $v(R)$ is cut off at $v = 1 - 1/(4N)$. N was 10. Simulation results for $N = 20$ yielded similar results (data not shown). The Fortran code containing the integrated models of the three papers is available upon request

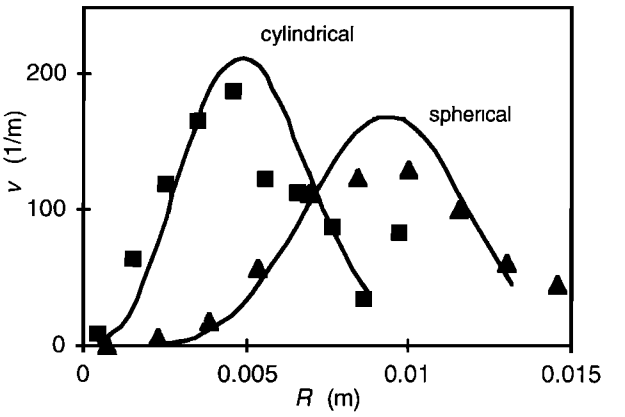

Figure 3. Weight function v for the radius R of the single-root model systems. Root density is 1 kg dw m^{-3} soil, SRL_{prim} is 4.5×10^3 m kg^{-1} dw, l_{lat} is 0.04 m; Δx_{lat} is 0.002 m and f_{prim}, is 0.22. Sources are in the work of *Segers and Leffelaar* [this issue (a, b)]. Symbols represent the numerical procedure (Appendix B) for the structured root systems with lateral roots attached to primary roots. The lines represent the analytical equation (4) for the random root systems with same total root (tip/length) density. The rather odd position of the square at the largest R (0.01 m) is due to the truncation of the function which goes to infinity.

3. Model Behavior

3.1. Description of Root System

Weight functions for system radius R, $v(R)$, were calculated for a number of illustrative cases (Figure 3). The analytical solutions (equation (4)) of the random root systems closely match the numerical calculations of root systems with the same root density (L_{tot} or N_{tot}) but a nonrandom geometry. Apparently, for the given root parameters the roots are effectively randomly distributed. This can be explained by the length of the lateral roots (40 mm), which is larger than typical distances between the primary roots (≈ 20 mm with the prevailing root parameters [*Segers and Leffelaar*, this issue (a), equations (A9)]. By contrast, if the length of the lateral roots is shorter than the distances between the primary roots (which may be the case in reed (with a high density of lateral roots [*Conlin and Crowder*, 1988]), for example) then the root system is clustered and the distance probability density distribution gets wider than the distribution of the randomly distributed roots (data not shown). As in our case, the difference between the two methods for estimating $v(R)$ is small; we used the fastest and simplest method, the analytical expression, in the remainder of the paper.

3.2. Full, Simplified and Homogeneous Model at the Soil Layer Level

The complete soil layer model with N-weighted single-root model systems is called the full soil layer model (equation (1)).

In the simplified soil layer model (equations (5) - (17)), the rates are calculated in two single-root model systems: an oxygen-unsaturated single-root model system and an oxygen-saturated single-root model system. To investigate the meaning of the single-root details of these models, also, an even more simple soil layer model was tested: the kinetic soil layer model. In this model, kinetic knowledge is directly applied at the soil layer level.

Simulations of relative aeration $\bar{\bar{\kappa}}$ are little affected by the assumptions in the simplified soil layer model, and also the homogeneous soil layer model results in only slightly higher aeration than the two other models (Figure 4a) due to the absence of the apparently small influence of oxygen-saturated single-root model systems in the homogeneous soil layer model. This means that in the full and in the simplified model,

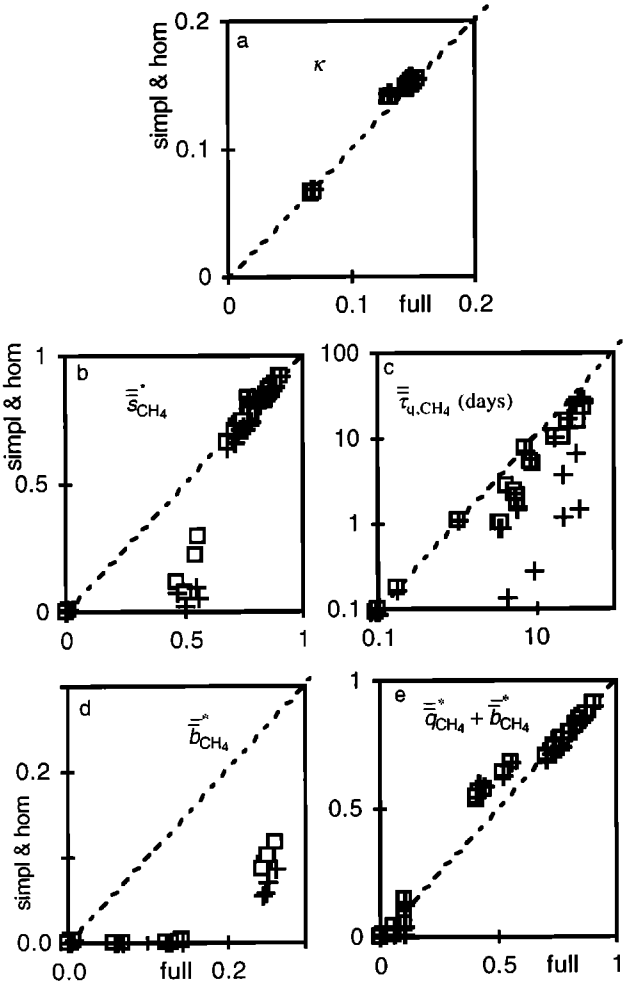

Figure 4. Comparison of simplified (open squares) and homogeneous (pluses) models with full model after 30 days for 32 different parameter sets. Parameter values are in the work of *Segers and Leffelaar* [this issue (a)], and in section 2.5. (a) O_2 supply/ O_2 demand, κ; (b) net normalised methane production $\bar{\bar{s}}^*_{CH_4}$; (c) time coefficient for methane release via plant $\bar{\bar{\tau}}_{q,CH_4}$; (d) normalized methane released via ebullition $\bar{\bar{b}}^*_{CH_4}$; and (e) total normalized methane release $\bar{\bar{b}}^*_{CH_4}+\bar{\bar{q}}^*_{CH_4}$. Methane production and methane release are normalized with $f_{an}\ v_{mg}\ s_{rcm}$, the maximum (equilibrium) methane production if no oxygen enters the system. The dashed line is the one-to-one line.

only a small part of the gas-exchanging root surface experiences a limited oxygen sink due to another root nearby.

Net methane production is lower in the homogeneous model and in the simplified model compared to the full model, especially when normalized net methane production is low (Figure 4b). Hence the nonlinear interactions among relative aeration κ, the relative oxygen sink strength ω, and net methane production s_{CH_4} at scales below the soil layer do have some impact on net methane production, and the use of effective values (equation (14)) introduces an inaccuracy. In process terms, methane production only occurs if all alternative electron acceptors are depleted. Averaging eliminates the spots with the very low concentrations of electron acceptors and hence reduces net methane production.

Time coefficients for methane transport through the roots, $\bar{\bar{\tau}}_{q,CH_4}$, $(\bar{\bar{c}}_{CH_4}/\bar{\bar{q}}_{CH_4})$ of the simplified soil layer model are smaller than those of the full soil layer model (Figure 4c). To investigate this difference, a simple analytical case study was carried out: an inert gas, with initial soil concentration $\bar{\bar{c}}_0$, is released to the atmosphere (concentration zero). According to the full soil layer model (equation (1)),

$$\bar{\bar{c}}(t) = \bar{\bar{c}}_0 \int_0^\infty v(R) \exp\left(-\frac{t}{\tau_q(R)}\right) dR, \qquad (20)$$

where $\bar{\tau}_q$ is the time coefficient of a single-root model system (increasing with R, equation (A24)). From equation (20) it is clear that the contribution to the total concentration of the single-root model systems with the largest radius increases in time. These single-root model systems could be seen as dead zones that exchange gases slowly with the atmosphere. By introducing an averaging procedure, these dead zones are artificially mixed with the remainder of the system, enhancing total transport and preventing the overall time coefficient $\bar{\bar{\tau}}_q$ to increase in time. Therefore plant-mediated transport is faster in the simplified models compared to the full model.

So a fundamental problem with methane release from the soil on the root system scale is that one needs to know the spatial microdistribution of methane, which depends on the history and which cannot be estimated from the actual average concentrations only. Consequently, gas-transport experiments with plants in a mixed culture solution [*Nouchi*, 1994; *Hosono and Nouchi*, 1997; *Butterbach-Bahl et al.*, 1997] cannot be directly extrapolated to the soil, and the first-order models [*Nouchi et al.*, 1994; *Hosono and Nouchi*, 1997; *Stephen et al.*, 1998; *Walter et al.* 1996] have to be interpreted with care.

Similar to methane plant transport, averaging reduces rates of bubble release (Figure 4d), firstly because of the nonlinear relation between bubble volume and bubble release (equation (A26)) and, secondly, because of the lower methane concentrations as a result of the higher plant-mediated transport. As the errors introduced by the assumptions on net methane production and methane transport partly cancel, the difference in simulated normalized methane flux by the full and the simplified model is surprisingly small (Figure 4e).

In the analysis above (Figures 4), variables were analyzed after 30 days, under constant driving variables. However, differences among the three models depend on simulation time (Figure 5). In situ driving variables, such as temperature and aeration (water table), will fluctuate on all kinds of timescales. Consequently, it is difficult to judge how large the difference

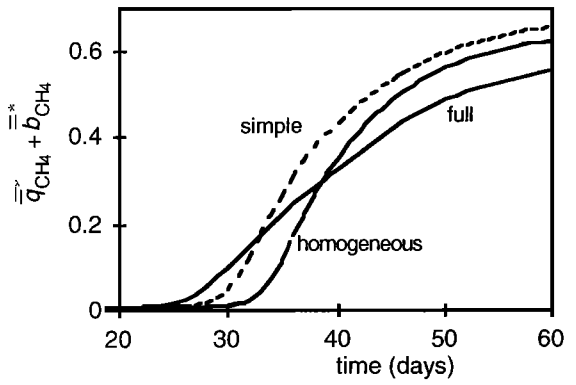

Figure 5. Comparison of simulated time courses of normalized methane emission by the homogeneous, simplified, and full models for parameter set 12. The three models are defined in the main text. Parameter values are in the work of *Segers and Leffelaar* [this issue (a)], and in section 2.5. Methane release is normalized with $f_{an}\ v_{mg}\ s_{rcm}$, the maximum (equilibrium) methane production if no oxygen enters the system.

among the homogeneous, the simplified, and the full model will be when incorporated in a model for fluxes at the plot scale. Therefore in paper 3 [*Segers and Leffelaar*, this issue (b)], which will address this scale, all three models will be used. In the remaining part of this paper, only the full soil layer model is used.

3.3. Cylindrical and Spherical Geometry

Two models for root and rhizosphere geometry were used: a cylindrical and spherical. The cylindrical model represents a situation where the whole root surface exchanges gases. The spherical model reflects the situation where only root tips are active. To compare both models, k_{rt} and ψ_{rt}'' are taken in such a way that total root activity per root dry weight is constant [*Segers and Leffelaar*, this issue (a), equation (A8)]. The difference in exchange area (determined by l_{lat} and r_{rt}) is a factor of 200, which is probably an upper value, as root radius is rather small (0.1 mm), and as in reality, the active area of a root is probably larger than the root tip only.

In the spherical case, transport between root surface and soil is more difficult than in the cylindrical, because the exchange surface is smaller in the spherical case. Consequently, aeration is lower (Figure 6a) and net methane production; the time coefficients for methane transport via the plant and total methane emission are higher in the spherical case (Figures 6b–6d). Because of the lower plant transport in the spherical case, ebullition is enhanced in the spherical case (Figure 6e). Also, the sensitivity of net methane production for the root gas-transport coefficient k_{rt} is much less in the spherical case compared to the cylindrical case (Figure 7), as in the first case oxygen release is more limited by the transport from the root surface to the soil. These differences in behavior can be understood in terms of the dimensionless number γ [*Segers and Leffelaar*, this issue (a)]. In the cylindrical case, γ is much smaller than 1, which means that in the cylindrical case, gas-transport directly around a root is not important. By contrast in the spherical case, γ is about 1, which means that gas-transport around a root is approximately as important as gas-transport within a root.

4. Model Applications

4.1. Relation of Methane Flux with Root Gas-Transport Coefficient

The root surface gas-transport coefficient k_{rt} has been varied over 2 orders of magnitude within the plausible range as estimated by *Segers and Leffelaar* [this issue (a)]. Net methane production was very sensitive for k_{rt}, especially in the cylindrical case (Figure 7). The extreme range in relative net methane production is not unrealistic as redox values in water-saturated soils with gas-transporting plants may vary between

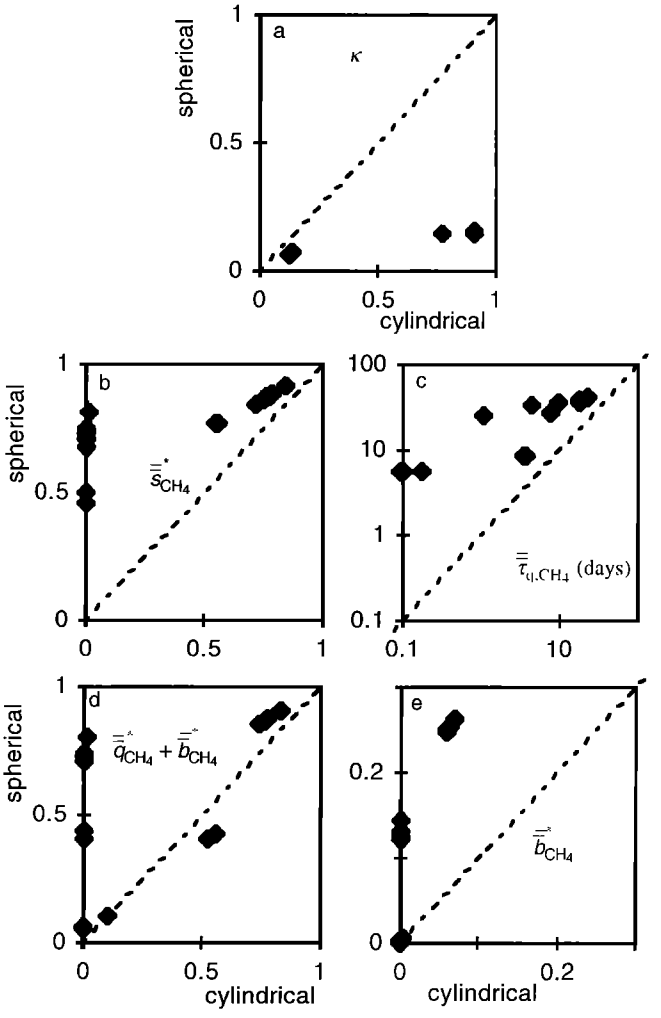

Figure 6. Difference between cylindrical and spherical geometry for 16 parameter sets after 30 days simulation time. Values k_{rt} and ψ_{rt}'' (which are on root surface basis) were set to keep potential root surface gas-transport constant on a root mass basis. Parameter values are in the work of *Segers and Leffelaar* [this issue (a)], and in section 2.5. (a) O_2 supply/ O_2 demand κ (only three points visible, because aeration was similar for many parameter sets); (b) net normalized methane production $\bar{\bar{s}}^{*}_{CH_4}$; (c) time coefficient for methane release via plant $\bar{\bar{\tau}}_{q,CH_4}$; (d) total normalised methane release $\bar{\bar{b}}_{CH_4}+\bar{\bar{q}}^{*}_{CH_4}$; and (e) normalised methane release only via transport of bubbles $\bar{\bar{b}}_{CH_4}$. Methane production and methane release are normalised with $f_{an}\ v_{mg}\ s_{rcm}$, the maximum (equilibrium) methane production if no oxygen enters the system. The dashed line is the one-to-one line.

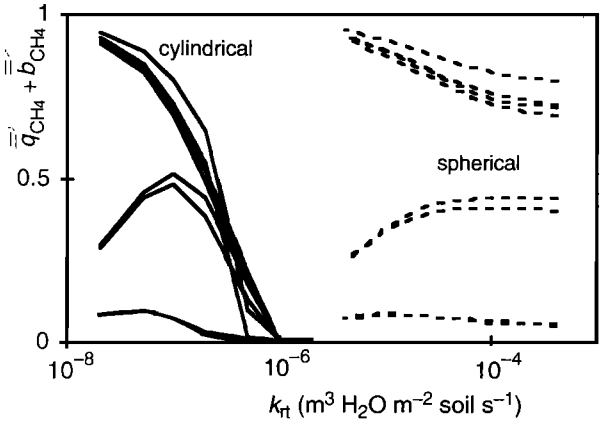

Figure 7. Normalized methane release $\bar{\bar{b}}_{CH_4}+\bar{\bar{q}}_{CH_4}$ as a function of root gas-transport coefficient k_{rt} for eight different parameter sets after 30 days of simulation. Parameter values are in the work of *Segers and Leffelaar* [this issue (a)], and in section 2.5. Methane release is normalized with f_{an} ν_{mg} s_{rcm}, the maximum (equilibrium) methane production if no oxygen enters the system.

−200 and +300 [*Holzapfel-Pschorn et al.*, 1986; *Chen and Barko*, 1988; *Grosse et al.*, 1996; *Frenzel et al.*, 1999].

Furthermore, it is interesting to note that k_{rt} may be both positively or negatively correlated with methane emissions. By contrast, *Arah and Stephen* [1998] found a consistently negative correlation between methane emissions and k_{rt}, because they considered the steady state of the system, whereas we evaluated emissions after 30 days simulation time. In our simulations, net methane production, which is equal to net methane emission in steady state, was consistently negatively correlated with k_{rt} (data not shown). In reality, all kinds of times are relevant, especially when a fluctuating water table is present. So, it is hard to draw general conclusion about the sensitivity of methane emissions for k_{rt}. Little information is available on exact values of k_{rt}, which means that knowledge on this parameter is one of the factors that limit the predictability of methane fluxes with a process model.

4.2. Relation of Methane Flux with Root Density

The model was run for a range of root densities for several combinations of sensitive parameters, with carbon availability (represented by s_{rcm}) proportional to root density. Potential methane oxidation was scaled with root density, as it is likely that roots promote the presence of both methane and oxygen, leading to higher active methanotrophic biomass.

At low root densities, net normalized methane production remains low, because after the 30 days simulation time the carbon availability is too low to reduce a substantial amount of the electron acceptors (Figure 8a). This may represent the situation in deep soil or an oligotrophic peat with mainly mosses. At higher root densities, net methane production normalized with s_{rcm} (and thus with root density (equation 19)) is independent of root density (Figure 8a). This implies that (not normalized) net methane production is proportional to root density, which is remarkable given the nonlinearities in the model.

In experiments with clipped or completely removed plants, soil methane concentrations sometimes decrease [*Whiting and Chanton*, 1992; *Waddington et al.*, 1996; *Yavitt*, 1997] and sometimes increase [*Yavitt*, 1997; *Verville et al.*, 1998; *King et al.*, 1998]. These manipulations may be seen as an artificial decrease of root density. In the model, decreasing root density consistently decreases soil methane concentrations (Figure 8b). This discrepancy between model and experiment may be due to a difference in the dependence of carbon mineralization on root density. In the model this dependence is assumed to be linear. However, in the experiments the dependence may be less than linear over the considered time, because soil carbon availability is not only

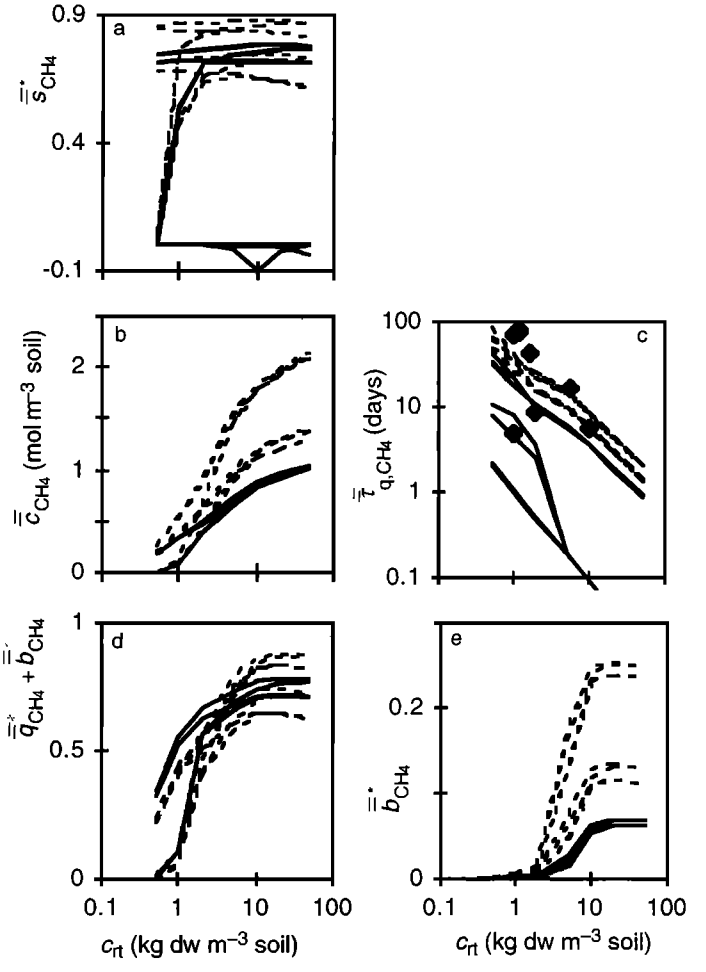

Figure 8. Model results as a function of root density, c_{rt}. Parameter values are in the work of *Segers and Leffelaar* [this issue (a), Table 3], and in subsection 2.5, apart from $Vm_{mo,mx}$, which was proportional to c_{rt}. (a) Net normalized methane production $\bar{\bar{s}}^{*}_{CH_4}$; (b) soil methane concentration $\bar{\bar{c}}_{CH_4}$; (c) time coefficient for methane release via the plant $\bar{\bar{\tau}}_{q,CH_4}$; (d) total methane release $\bar{\bar{b}}_{CH_4}+\bar{\bar{q}}^{*}_{CH_4}$; and (e) methane release via ebullition $\bar{\bar{b}}_{CH_4}$. Methane production and methane release are normalized with f_{an} ν_{mg} s_{rcm}, the maximum (equilibrium) methane production if no oxygen enters the system. Solid lines are with the cylindrical geometry, dashed lines with the spherical geometry. Diamonds in Figure 8c are from experiments with soil cores with bog bean [*Stephen et al.*, 1998]. Note that as result of the parameterization, the normalization variable s_{rcm} is proportional to c_{rt}.

dependent on the vegetation of the near past. Hence information on soil carbon flows is needed to properly interpret vegetation removal experiments.

The dependence of the time constant of root gas-transport on root density is similar to the experimental findings for bog bean (Figure 8c). The simulations show that at higher root densities, methane emission is proportional to root density (Figure 8d), which confirms the experimentally found linear relations between methane fluxes and biomasses of grasses and sedges [*Whiting et al.*, 1991; *van den Pol-van Dasselaar*, 1999]. The disproportionate relation at lower root densities can be explained by (1) the effective time coefficient of plant gas-transport being larger than the simulation time at low root densities (Figure 8c) and by (2) the onset of ebullition at high root densities (Figure 8e) when methane concentrations are high enough.

4.3. Possible Model Extensions

The knowledge from the single-root level is scaled up to the soil layer level by a probability density distribution for R. By contrast, other system parameters are assumed to be constant within a soil layer. However, it is probable that apart from R, also k_{rt} and s_{rcm} vary within a soil layer, because parts of the roots will be more effectively connected to the atmosphere than other parts and as hot spots will be present in which carbon is preferentially available. It would be possible to assume probability density distributions for k_{rt} and s_{rcm} as well. However, this would make interpretation of results more complex without an increase in predictability on the field scale, as information on average or effective values of k_{rt} and s_{rcm} is scarce, let alone information on the variation in these parameters.

In the model and the sensitivity analysis it was assumed that most parameters are independent. Only $\omega_{mo,mx}$ was scaled with c_{rt}. However, also other parameters are probably correlated to each other. If redox decreases, plants tend to increase their gas-transport capacity by increasing root oxygen release to prevent damage by toxic compounds [*Drew and Lynch*, 1980; *Kludze et al.*, 1993; *Kludze and Delaune*, 1996]. So probably high ψ''_{rt} is correlated to high values of k_{rt}. Principally, it would be possible to dynamically model such an adaptation mechanism by relating the rate of change of k_{rt} to, for example, the oxygen concentration at the root surface. However, practically, this would be difficult because quantitative information on such relations is absent. A functional relation, assuming sufficient adaptation, is also not feasible, because the actual redox conditions in rooted water-saturated soil may vary largely [*Chen and Barko*, 1988; *Holzapfel-Pschorn et al.*, 1986; *Grosse et al.*, 1996]. So quantitative research on plant-mediated transport and its regulating mechanisms [*Jackson and Armstrong*, 1999] is needed to be able to predict k_{rt} under various circumstances.

As a first approach, it was assumed that the root system is static. Given the large time coefficient of root turnover, this may seem realistic. However, in reality, root growth and inactivation of root oxygen loss may occur in short time intervals (a month [*Hines et al.*, 1989; *Behaeghe*, 1979]) in the season. Fast root dynamics may have two implications. Firstly, the probability density function of the model systems will be dynamic and, secondly a kind of mixing will occur, because aerobic spots (new roots) will emerge at anaerobic spots and aerobic spots (decaying roots) will emerge in anaerobic spots. This mixing may be described with an exchange between the different single-root model systems or an exchange between the shells of different single-root model systems.

5. Concluding Remarks

In this paper we scaled up from the single-root scale to the soil layer scale. The simulation results demonstrate that methane emission may be limited by several processes (oxygen transport via vegetation, root oxygen consumption, methane transport via vegetation, reduction of electron acceptors, soil carbon mineralization). The relative importance of these processes depends on the conditions. For example, at high root densities (>2 kg dw m^{-3}), under continuous water saturation and at longer times (months/years), methane emission is proportional to root density, whereas at short times (days/weeks), reduction of electron acceptors may be limiting, and at intermediate times (weeks/months) and modest root densities (1 kg dw m^{-3}), gas-transport via the vegetation may be crucial.

Appendix A: Overview of Simplified Single Root Model

The simplified single-root model was derived from the full single-root model, which is a coupled set of root reaction-diffusion equations for methane, oxygen, molecular nitrogen, carbon dioxide, and electron acceptors in oxidized (eo) and reduced (er) form [*Segers and Leffelaar*, this issue (a), equations (2)-(33)]. The equations were simplified in two steps: (1) quasi-steady-state assumption for oxygen, and (2), spatially averaging the equations for the other state variables. The result of this procedure is a set of coupled ordinary differential equations for the mean concentrations, $\bar{c}$:

$$\frac{d\bar{c}_{CH_4}}{dt} = \bar{s}_{CH_4} + \bar{q}_{CH_4} + \bar{b}_{CH_4}, \tag{A1}$$

$$\frac{d\bar{c}_{CO_2}}{dt} = \bar{s}_{CO_2} + \bar{q}_{CO_2} + \bar{b}_{CO_2}, \tag{A2}$$

$$\frac{d\bar{c}_{N_2}}{dt} = \bar{q}_{N_2} + \bar{b}_{N_2}. \tag{A3}$$

$$\frac{d\bar{c}_{eo}}{dt} = \bar{s}_{eo}. \tag{A4}$$

$$\frac{d\bar{c}_{er}}{dt} = \bar{s}_{er}. \tag{A5}$$

Here $\bar{s}$ is the spatially averaged kinetic rate, $\bar{q}$ is the spatially averaged gas-transport via the plant, and $\bar{b}$ is the spatially averaged gas-transport via bubbles.

Net methane production is the result of methane production (mg) and methane oxidation (mo):

$$\bar{s}_{CH_4} = \bar{s}_{mg,CH_4} + \bar{s}_{mo\,CH_4}. \tag{A6}$$

Electron acceptor cycling is the result of electron acceptor reduction (rd) and electron acceptor reoxidation (ro).

$$\bar{s}_{eo} = \bar{s}_{rd,eo} + \bar{s}_{ro,eo}, \tag{A7}$$

$$\bar{s}_{er} = \bar{s}_{rd,er} + \bar{s}_{ro,er}, \tag{A8}$$

and carbon dioxide production is the result of aerobic respiration (ae), methane oxidation, electron acceptor reduction, and methane production:

$$\bar{s}_{CO_2} = \bar{s}_{ae,CO_2} + \bar{s}_{mo,CO_2} + \bar{s}_{rd,CO_2} + \bar{s}_{mg,CO_2}. \quad (A9)$$

Two groups of processes are distinguished: aerobic processes and anaerobic processes. To compare the different processes, all rates were normalized with carbon mineralization under optimal aeration or with the oxygen demand for this process.

A1. Aerobic Processes

The aerobic processes (aerobic respiration, methane oxidation, and electron acceptor reoxidation) are determined by the total oxygen consumption $\bar{s}_{O_2}$, and the relative oxygen sink strengths ω of each process:

$$\bar{s}_{ae,O_2} = \frac{\bar{\omega}_{ae}}{\bar{\omega}} \bar{s}_{O_2}, \quad (A10)$$

$$\bar{s}_{mo,O_2} = \frac{\bar{\omega}_{mo}}{\bar{\omega}} \bar{s}_{O_2}, \quad (A11)$$

$$\bar{s}_{ro,O_2} = \frac{\bar{\omega}_{ro}}{\bar{\omega}} \bar{s}_{O_2}. \quad (A12)$$

By definition, ω is the oxygen sink relative to the oxygen sink for aerobic respiration:

$$\bar{\omega} \equiv \bar{\omega}_{ae} + \bar{\omega}_{mo} + \bar{\omega}_{ro}, \quad (A13)$$

$$\bar{\omega}_{ae} \equiv 1, \quad (A14)$$

$$\bar{\omega}_{mo} \equiv \frac{\nu_{mo}\, Vm_{mo}}{\nu_{ae}\, s_{rem}} \frac{\bar{c}_{aq\,CH_4}}{\bar{c}_{aq\,CH_4} + K_{mo,CH_4}}, \quad (A15)$$

$$\bar{\omega}_{ro} \equiv \frac{\nu_{ro}\, k_{ro}\, \theta\, \bar{c}_{aq,er}}{\nu_{ae}\, s_{rem}} \quad (A16)$$

The total oxygen consumption rate $\bar{s}_{O_2}$ is calculated from steady state solution of the reaction-diffusion equation for oxygen, assuming a zero-order behavior. The essential property of the procedure is that root oxygen release (equal to total oxygen consumption) depends on only two dimensionless numbers:

$$\beta \equiv \frac{k_{rt}\left(\alpha\, c_{g,atm,O_2} - \frac{\psi_{rt}''}{k_{rt}}\right)}{\nu_{ae}\, \omega\, s_{rem}\, r_{rt}}, \quad (A17)$$

$$\gamma \equiv \frac{k_{rt}\, r_{rt}}{D_{aq,eff}}. \quad (A18)$$

In both numbers k_{rt} appears, which is the root surface transport coefficient for gases, used as boundary condition at the root surface in the original reaction-diffusion equation:

$$\phi'' = k_{rt}\left(\alpha\, c_{g,atm}\left(1 - \frac{\psi_{rt}''}{k_{rt}\alpha\, c_{g,atm}}\right) - c_{aq,rt}\right). \quad (A19)$$

Here $\alpha\, c_{g,atm}$ is the aqueous gas concentration in equilibrium with the atmosphere, $[c_{rt}]$ is the gas concentration at the root surface, and ψ_{rt}'' is the root oxygen consumption, assumed to be completely at the root surface. The aerobic rates of change in methane, carbon dioxide, and electron acceptors are related to the oxygen consumption rates (equations (A10)-(A12)) via stoichiometric factors (relations not shown).

A2. Anaerobic Processes

Both anaerobic processes (methane production and electron acceptor reduction) are determined by anaerobic C-mineralization ($\bar{s}_{acm}$),

$$\bar{s}_{mg,CH_4} = \nu_{mg}\, \bar{\zeta}_{mg}\, \bar{s}_{acm}, \quad (A20)$$

$$\bar{s}_{rd,co} = -\nu_{rd}\,(1 - \bar{\zeta}_{mg})\, \bar{s}_{acm}. \quad (A21)$$

The fraction of anaerobically mineralized carbon that ends up in methanogenesis (ζ_{mg}), depends on the kinetic constants and the concentration of electron acceptors. If ample electron acceptors are present, methane production is low, and ζ_{mg} approaches zero. When the electron acceptors get depleted, ζ_{mg} will rise toward 1. Anaerobic production of CO_2 and reduced electron acceptors depend on equations (A20) and (A21) via stoichiometric relations (not shown).

Anaerobic C-mineralization could be related to the aerobic processes, for which expressions are above,

$$\bar{s}_{acm} = f_{an}\, s_{rem}\left(1 - \frac{\bar{s}_{O_2}}{\omega\, \nu_{ae}\, s_{rem}}\right). \quad (A22)$$

Here f_{an} is a factor that describes the reduction of C-mineralization under anaerobic conditions compared to aerobic conditions.

A3. Root Gas Transport of Gases Other Than Oxygen

Plant-mediated transport of gases other than O_2 is modeled with a first-order relation:

$$\bar{q}_t = -r_{q,t}\,(\bar{c}_{aq,t} - \alpha_t\, c_{g,atm,t}), \quad (A23)$$

where $c_{g,atm,t}$ is the gas concentration in the atmosphere of gas t. The first-order constants $r_{q,t}$ were taken from the steady state solution of the reaction-diffusion equation with methane production constant in time and space:

$$r_{q,c,t} = \frac{2\, k_{rt}}{r_{rt}} \left(\frac{r_{rt}}{R}\right)^2 \frac{1}{\left(1 + \gamma_t \ln\left(\frac{R}{r_{rt}}\right)\right)}, \quad (A24a)$$

$$r_{q,s,t} = \frac{3\, k_{rt}}{r_{rt}} \left(\frac{r_{rt}}{R}\right)^3 \frac{1}{(1+\gamma_t)}. \quad (A24b)$$

A4. Bubble Transport

Ebullition is calculated in two steps. First the bubble volume ε_{bub} is calculated from the equilibrium equations between the gas and the aqueous phase for all gases:

$$\sum_t \frac{\frac{\bar{c}_t}{c_{sat,t}}}{1 - \varepsilon_{solid} - \bar{\varepsilon}_{bub}\left(1 - \frac{1}{\alpha_t}\right)} = 1. \quad (A25)$$

Subsequently, bubble release is assumed to rise sharply after a critical bubble volume ε_{cr}, using an expolinear equation:

$$\bar{b}_t = -\frac{\nu_{bub}}{\Delta z\, curv\, \varepsilon_{cr}} \ln(1 + \exp(curv\,(\bar{\varepsilon}_{bub} - \varepsilon_{cr})))\, \bar{c}_{g,t}. \quad (A26)$$

Appendix B: Weight Functions for the Spherical Case

In analogy with the derivations of *Rappoldt* [1992, equation (7.1)] for a cylinder the distribution of the distance to the gas exchanging surface in a single sphere with radius R is equal to the surface to volume ratio:

$$g_s(R, x) = \frac{4\pi x^2}{4/3\,\pi R^3} = \frac{3x^2}{R^3} \quad 0 \le x \le R, \qquad g_s(R, x) = 0 \quad x > R \tag{B1}$$

Then the distance probability distribution for a set of spheres with weight function $v_s(R)$ becomes (in analogy with *Rappoldt* [1992, equation (7.5)])

$$g_s(x) = \int_0^\infty g_s(R, x)\, v_s(R)\, \mathrm{d}R = \int_x^\infty \frac{3x^2}{R^3} v_s(R)\, \mathrm{d}R = 3x^2 \int_x^\infty \frac{1}{R^3} v_s(R)\, \mathrm{d}R. \tag{B2}$$

Substitution of equation (B2) into the derivative of equation (B2) with respect to x leads to an expression of v_s as function of $g_s(x)$.

$$v_s(R) = \frac{2}{3} g_s(x) - \frac{1}{3} x \frac{\mathrm{d}g_s(x)}{\mathrm{d}x}\Big|_{x=R}. \tag{B3}$$

To find a discretized form of equation (B3), the starting point is the discretized equivalent of equation (B2):

$$p_i = \sum_{m=1}^{nm} P_{i,m}\, w_{s,m}, \tag{B4}$$

where p_i is the probability that x is in distance class i, and $P_{i,m}$ is the probability that a point of the model system with radius R_m is in distance class i. If there are N equal distance classes and if the model systems consists of N spheres with radii equal to the upper bounds of the distance classes, then in analogy with [*Rappoldt*, 1992, equations (7.22) and (7.25)]

$$P_{i,m} = \int_{x_{i-1}}^{x_i} \frac{3x^2}{R_m^3}\,\mathrm{d}x = \frac{x_i^3 - x_{i-1}^3}{R_m^3} = \frac{3i^2 - 3i + 1}{m^3} \quad i \le m, \tag{B5a}$$

$$P_{i,m} = 0 \quad i > m. \tag{B5b}$$

Combining equations (B4) and (B5) leads, via back substitution [*Press et al.*, 1987, p. 30], to

$$w_{s,N} = \frac{N^3}{3N^2 - 3N + 1} p_N, \tag{B6a}$$

$$w_{s,m} = \frac{m^3}{3m^2 - 3m + 1}\left(p_m - (3m^2 - 3m + 1) \sum_{i=m+1}^{N} \frac{1}{i^3} w_{s,i}\right) \quad m < N. \tag{B6b}$$

Appendix C: PDF of Distance to Nearest Root of Root System With Lateral Roots Attached to Randomly Distributed Primary Roots

Lateral roots constitute the largest part of the root length density, and it is probable that these roots release the largest part of the oxygen. Therefore an adequate description of the geometry of lateral roots is needed to obtain a realistic model of rhizosphere aeration. Lateral roots are not randomly distributed, as they are attached to primary roots. To study this, an artificial 3-D root system is generated.

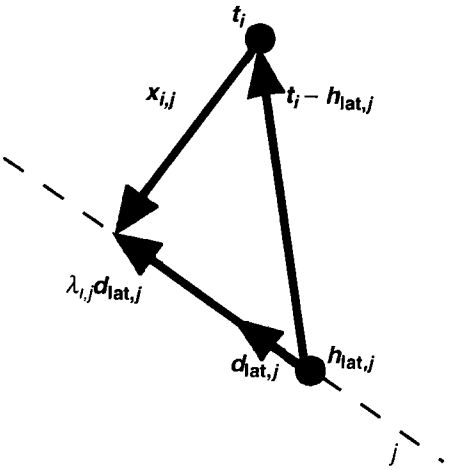

Figure C1. Illustration for the calculation of the distance between the test point t_i and the lateral root, characterized by a base vector $\boldsymbol{h}_{\mathrm{lat},j}$, a direction vector $\boldsymbol{d}_{\mathrm{lat},j}$ and a length l_{lat} (not in the graph). $\boldsymbol{x}_{i,j}$ is the vector between the test point t_i and the nearest point on line j (dashed).

To represent the primary roots, a set of random lines is generated in sphere (radius R_{rtsys}) with root length density L_{prim}, using *Rappoldt* [1993, equations (9)-(11)]. R_{rtsys} was 10 times the length scale of the primary root system ($1/\sqrt{L_{\mathrm{prim}}}$). At each Δx_{lat}, lateral roots with constant length l_{lat} are attached to the primary roots. Each lateral root is represented by a base vector $\boldsymbol{h}_{\mathrm{lat}}$, which lies on a primary root, and a direction vector $\boldsymbol{d}_{\mathrm{lat}}$, which lies in the plane perpendicular to the primary root. The orientation in the plane is random.

Subsequently, random test points $\boldsymbol{t}_i$ are generated within the sphere. The number of test points was so high (10,000) that the results were not affected by further increasing this number. $\boldsymbol{x}_{i,j}$ is the vector between the test point $\boldsymbol{t}_i$ and the nearest point on the line j defined by $\boldsymbol{h}_{\mathrm{lat},j}$ and $\boldsymbol{d}_{\mathrm{lat},j}$ (Figure C1). $\boldsymbol{x}_{i,j}$ and $\boldsymbol{d}_{\mathrm{lat},j}$ are perpendicular:

$$\boldsymbol{x}_{i,j} \cdot \boldsymbol{d}_{\mathrm{lat},j} = 0, \tag{C1}$$

and the sum of the vectors of the triangle in Figure C1 is zero:

$$\boldsymbol{t}_i - \boldsymbol{h}_{\mathrm{lat},j} + \boldsymbol{x}_{i,j} - \lambda_{i,j}\, \boldsymbol{d}_{\mathrm{lat},j} = 0, \tag{C2}$$

where $\lambda_{i,j}$ is distance between $\boldsymbol{h}_{\mathrm{lat},j}$ and the end of $\boldsymbol{x}_{i,j}$. Here note that the length of the direction vector $\boldsymbol{d}$ is 1. Taking the inproduct with $\boldsymbol{d}_{\mathrm{lat},j}$ for all the terms of equation (C2) and using equation (C1) results in

$$\lambda_{i,j} = (\boldsymbol{t}_i - \boldsymbol{h}_{\mathrm{lat},j}) \cdot \boldsymbol{d}_{\mathrm{lat},j}. \tag{C3}$$

The lateral root is present at only a part of the line j. If $\lambda_{i,j} < 0$, then the nearest point of the lateral root to the test point is at the base of the lateral root, and hence, the distance of test point $\boldsymbol{t}_i$ to the lateral root j is $|\boldsymbol{t}_i - \boldsymbol{h}_{\mathrm{lat},j}|$. If $\lambda_{i,j}$ is between zero and l_{lat}, then the distance of test point $\boldsymbol{t}_i$ is equal to $|\boldsymbol{t}_i - (\boldsymbol{h}_{\mathrm{lat},j} + \lambda_{i,j}\, \boldsymbol{d}_{\mathrm{lat},j})|$, otherwise it is equal to $|\boldsymbol{t}_i - (\boldsymbol{h}_{\mathrm{lat},j} + l_{\mathrm{lat}}\, \boldsymbol{d}_{\mathrm{lat},j})|$.

Notation

b rate of change in soil gas concentration due to bubble release from a soil volume, mol m^{-3} soil s^{-1}.

c soil concentration of gas or solute, mol m^{-3} soil.
$\boldsymbol{c}$ concentrations in soil of all gases and solutes, mol m^{-3} soil.
c_0 initial concentration, mol m^{-3} soil.
c_{rt} root density in soil, kg dw m^{-3} soil.
c_{sat} saturated aqueous gas concentration, mol m^{-3} H_2O.
curv curvature of equation for bubble release (equation (A26)), m^3 soil m^{-3} gas.
$\boldsymbol{d}_{lat,j}$ direction vector of lateral root j, m.
$D_{aq,eff}$ effective aqueous diffusion coefficient, m^3 H_2O m^{-1} soil s^{-1}.
f_{an} reduction factor that describes the rate of anaerobic C-mineralization relative to the rate of aerobic C-mineralization.
f_C mass fraction of carbon in roots.
f_{prim} mass fraction of primary roots, kg dw primary root kg^{-1} dw total root.
$g(x)$ probability density of distance to nearest root, m^{-1}.
$\boldsymbol{h}_{lat}$ base vector of lateral root, m.
k_{ro} rate constant for electron acceptor reoxidation, s^{-1}.
k_{rt} effective root surface gas-transport coefficient, m^3 H_2O m^{-2} soil s^{-1}.
$K_{p,i}$ half-saturation constant of process p and compound i, mol m^{-3} H_2O.
l_{lat} length of lateral root, m.
L_{prim} root length density of primary roots, m root m^{-3} soil.
L_{tot} root length density, m root m^{-3} soil.
M_C molar weight of carbon, kg mol^{-1}.
N_{tot} root tip density (number of root tips per volume of soil), m^{-3} soil.
N number of single-root model systems.
p_i probability that x, distance to nearest root, is in distance class i.
$P_{i,m}$ probability that a point of the model system m is in distance class i.
q rate of change in soil gas concentration due to transport of gas via plant, mol m^{-3} soil s^{-1}.
Q_{10} relative increase in activity upon a 10°C increase in temperature.
r_q effective root gas-transport coefficient, proportionality between rate of change of soil gas concentration due to vegetation-mediated gas transport and difference in aqueous gas concentration between atmosphere and soil, m^3 H_2O m^{-3} soil s^{-1}.
r_{rt} root radius, m.
R radius of single-root model system, m.
$R_{aer,0}$ outer spatial coordinate of aerated area around a root if aerobic respiration is the only O_2 sink in the soil, m.
R_{rtsys} radius of numerically generated root system, m.
s net production of a compound, mol m^{-3} s^{-1}.
SRL specific root length, m kg^{-1}.
t time, s.
$\boldsymbol{t}_i$ spatial coordinates of test point i, m.
T temperature, K.
T_{ref} reference temperature of Q_{10} factor, K.
v probability density of R, m^{-1}.
v_{bub} velocity of upward moving bubbles, m^3 gas m^{-2} soil s^{-1}.
$Vm_{p,i}$ maximum rate of process p and compound i, mol m^{-3} s^{-1}.
w_m weight of single-root model system m.
x distance to nearest root, m.
$\boldsymbol{x}_{i,j}$ vector between test point i and nearest point on the line through lateral root j, m.
α solubility, m^3 gas m^{-3} H_2O.
β ratio of time constants of O_2 sink in the soil and O_2 transport in the root.
β_0 β when aerobic respiration is the only O_2 sink in soil.
γ ratio of time constants of transport in the root and transport just around a root.
Δx_{lat} distance between the bases of the lateral root at the primary roots, m.
Δz thickness of soil layer, m.
ε_{bub} volumetric bubble content, m^3 gas m^{-3} soil.
ε_{cr} critical volumetric gas content for bubble release, m^3 gas m^{-3} soil.
ε_{solid} volumetric solid phase, m^3 solid m^{-3} soil.
ζ_{mg} fraction of anaerobically mineralized carbon which ends up in methanogenesis, the remaining fraction ends up in reduction of electron acceptors.
η_{aer} fraction of single-root model systems which is completely aerated.
θ volumetric moisture content, m^3 H_2O m^{-3} soil.
κ root O_2 release relative to the O_2 demand for aerobic respiration.
$\lambda_{i,j}$ location on the line j where vector $\boldsymbol{x}_{i,j}$ ends, m.
ν stoichiometric constant, mol mol^{-1}.
τ_q time constant of transport via plant, s.
τ_{rt} time constant of root turnover, s.
χ arbitrary quantity.
ψ_{rt}^{*} root respiration per gas exchanging root area, mol O_2 m^{-2} active area s^{-1}.
ω O_2 sink relative to O_2 sink for aerobic respiration.

Compounds

eo electron acceptor.
er reduced electron acceptor.
e_{tot} sum of oxidized and reduced electron acceptors.

Subscripts

acm anaerobic C-mineralization.
atm atmospheric.
c cylindrical.
g gas phase.
i index of compound, index of distance class.
j index of lateral root.
ae aerobic respiration.
lat lateral root.
m index of single-root model system.
mg methanogenesis.
mo methanotrophic.
mx maximum.
prim primary root.
rcm reference C-mineralization.
rd reduction of electron acceptors.
ro reoxidation of electron acceptors.
rt root.
s spherical.

Other Symbols

bold vector.
$\bar{}$ spatially averaged at the single-root level.
$=$ spatially averaged at the soil layer level.
* normalized with equilibrium CH_4 production when O_2 inflow is zero.

single-root systems that are completely aerated.
‡ single-root systems that are not completely aerated.

Acknowledgments. We thank Peter van Bodegom and Rudy Rabbinge for providing useful comments on a draft of this paper This research was financially supported by the Dutch National Research Programme on Global Air Pollution and Climatic Change (NRP-II).

References

Arah, J. R. M , and K. D. Stephen, A model of the processes leading to methane emission from peatland, *Atmos Environ , 32*, 3257-3264, 1998.

Behaeghe, T. J., *De seizoensvariatie in de grasgroei*, Fakult. Landbouwwetensch., Lab Landbouwplantenteelt en Herbologie, Rijksuniv Gent, Belgium, 1979.

Bellisario, L M , J L. Bubier, T. R. Moore, and J. P Chanton, Controls on CH4 emissions from a northern peatland, *Global Biogeochem Cycles, 13*, 81-91, 1999

Bird, R. B , W. E Stewart, and E N. Lightfoot, *Transport Phenomena*, 780 pp., John Wiley, New York, 1960.

Bridgham, S. D., K. Updegraff, and J. Pastor, Carbon, nitrogen, and phosphorus mineralization in northern wetlands, *Ecology, 79*, 1545-1561, 1998.

Butterbach-Bahl, K , H Papen, and H Rennenberg, Impact of gas-transport through rice cultivars on methane emission from rice paddy fields, *Plant Cell Environ , 20*, 1175-1183, 1997.

Chen, R. L , and J. W Barko, Effects of microphytes on freshwater ecology, *J. Freshwater Ecol., 4*, 279-289, 1988.

Clymo, R S , The limits to peat bog growth, *Philos. Trans R. Soc. London , ser B , 303*, 605-654, 1984

Conlin, T. S , and A. A. Crowder, Location of radial oxygen loss and zones of potential iron uptake in a grass and two nongrass emergent species, *Can J Bot., 67*, 717-722, 1988.

Conrad, R . Mechanisms controlling methane emission from wetland rice fields, in *Biogeochemistry of Global Change*, edited by R. S. Oremland, pp. 317-335, Chapman and Hall, New York, 1993.

Drew, M. C., and J. M. Lynch, Soil anaerobioisis, microorganisms, and root function, *Annu. Rev. Phytopathol., 18*, 37-66, 1980

Frenzel, P . U Bosse, and P H. Janssen, Rice roots and methanogenesis in a paddy soil Ferric iron as an alternative electron acceptor in the rooted soil, *Soil Biol. Biochem., 31*, 421-430, 1999

Fukuzaki, S. N., N. Nishio, and S. Nagai, Kinetics of methanogenic fermentation of acetate, *Appl. Environ Microbiol., 56*, 3158-3163, 1990.

Grosse, W , K Jovy, and H. Tiebel. Influence of plants on redox potential and methane production in water-saturated soil, *Hydrobiologia, 340*, 93-99, 1996.

Hines, M. E., Knollmeyer, L S , and Tugel, J B , Sulfate reduction and other sedimentary biogeochemistry in a northern New England salt marsh, *Limnol. Oceanogr , 34*, 578-590, 1989

Holzapfel-Pschorn, A., R. Conrad, and W. Seiler, Effects of vegetation on the emission of methane from submerged paddy soil, *Plant Soil, 92*, 223-233, 1986.

Hosono. T., and I. Nouchi, The dependence of methane transport in rice plants on the root zone temperature, *Plant Soil, 191*, 233-240, 1997

Jackson, M. B., and W Armstrong, Formation of Aerenchyma and the processes of plant ventilation in relation to soil flooding and submergence, *Plant Biol , 1*, 274-287, 1999

King, J. Y , W. S. Reeburgh, and S K. Regli, Methane emission and transport by arctic sedges in Alaska. Results of a vegetation removal experiment, *J Geophys Res., 103*, 29,083-29,092, 1998

Kludze, H K , and R. D. Delaune, Soil redox intensity effects on oxygen exchange and growth of cattail and sawgrass, *Soil Sci Soc. Am J , 60*, 616-621, 1996

Kludze, H. K., R. D. DeLaune, and W. H. Patrick, Aerenchyma formation and methane and oxygen exchange in rice, *Soil Sci. Soc Am J., 57*, 386-391, 1993

Nouchi, I , Mechanisms of methane transport through rice plants, in *CH4 and N2O: Global Emissions and Controls from Rice Fields and Other Agricultural and Industrial Sources*, edited by K. Minami, A. Mosier, and R. Sass , pp 87-104, Nation Inst. Agro-Environ. Sci., Tokyo, 1994.

Nouchi. I , T. Hosono, K Aoki, and K Minami, Seasonal variation in methane flux from rice paddies associated with methane concentration in soil water, rice biomass and temperature, and its modeling, *Plant Soil, 161*, 195-208 , 1994

Nykanen, H , J. Alm, J Silvola, K Tolonen, and P J Martikainen, Methane fluxes on boreal peatlands of different fertility and the effect of long-term experimental lowering of the water table on flux rates, *Global Biogeochem Cycles, 12*, 53-69, 1998.

Ogston, A G , The spaces in a uniform random suspension of fibres, *Trans Farraday Soc., 54*, 1754-1757, 1958.

Pielou, E C., *Mathematical Ecology*, 385 pp., John Wiley, New York, 1977

Prather, M., R. Derwent, D. Ehhalt, P. Fraser, E. Sanhueza, and X. Zhou, Other trace gases and atmospheric chemistry, in *Climate Change 1994. Radiative Forcing of Climate Change and an Evaluation of the IPCC IS92 Emissions Scenarios*, edited by J. T. Houghton, L. G Meira Filho, J. Bruce, H. Lee, B A. Callander, E. Haites, and K. Maskell, pp. 73-126, Cambridge Univ. Press, New York, 1995.

Press, W H , B P. Flannery, S. A Teukolsky, and W T Vetterling, *Numerical Recipes. The Art of Scientific Computing*, 3rd. ed., 818 pp., Cambridge Univ. Press, New York, 1987.

Rappoldt, C , The application of diffusion models to an aggregated soil, *Soil Sci , 150*, 645-661, 1990.

Rappoldt, C , Diffusion in aggregated soil, Ph.D. thesis, Wageningen Agric Univ., Wageningen, Netherlands, 1992.

Rappoldt, C , Modeling the geometry of a worm burrow system in relation with oxygen diffusion, *Geoderma, 57*, 69-88, 1993

Saarinen, T., Biomass and production of two vascular plants in a boreal mesotrophic fen, *Can. J. Bot., 74*, 934-938, 1996

Segers, R., Methane production and methane consumption, a review of processes underlying wetland methane fluxes, *Biogeochemistry, 41*, 23-51, 1998.

Segers, R , and P. A. Leffelaar, Modeling methane fluxes in wetlands with gas-transporting plants, 1, Single-root scale, *J Geophys. Res.*, this issue (a)

Segers, R , and P. A Leffelaar, Modeling methane fluxes in wetlands with gas-transporting plants, 3, Plot scale, *J. Geophys. Res* , this issue (b)

Shaver, G. R., and W. D. Billings, Root production and root turnover in a wet tundra ecosystem, Barrow, Alaska, *Ecology, 56*, 401-410, 1975.

Stephen, K. D., J. R. M. Arah, W Daulat, and R S. Clymo, Root mediated gas-transport in peat determined by argon diffusion, *Siol. Biol Biochem , 30*, 501-508, 1998

van den Pol-van Dasselaar, A., M. L. van Beusichem, and O. Oenema, Determinants of spatial variability of methane emission from wet grasslands on peat soil in a nature preserve, *Biogeochemistry, 44*, 221-237, 1999

Verville, J. H., S. E Hobbie, F. S. Chapin, and D U. Hooper, Response of tundra CH_4 and CO_2 flux to manipulation of temperature and vegetation, *Biogeochemistry, 41*, 215-235, 1998

Waddington, J. M., N T. Roulet, and R V. Swanson, Water table control of CH_4 emission enhancement by vascular plants in boreal peatlands, *J. Geophys Res., 101*, 22,775-22,785, 1996.

Wallén, B , Above and below ground dry mass of the three main vascular plants on hummocks on a subarctic bog, *Oikos, 46*, 51-56, 1986

Walter, B. P , M Heimann, R. D Shannon, and J R White, A process-based model to derive methane emissions from natural wetlands, *Geophys Res Lett., 23*, 3731-3734, 1996.

Wang, Z P , D Zeng, and W H. Patrick, Methane emissions from natural wetlands, *Environ Monit Assess , 42*, 143-161, 1996

Whiting, G J., and J P Chanton, Plant-dependent CH_4 emission in a subarctic Canadian fen, *Global Biogeochem Cycles, 6*, 225-231, 1992

Whiting, G J , J. P Chanton, D S. Bartlett, and J. D. Happell, Relationships between CH_4 emission, biomass, and CO_2 exchange in a subtropical grassland, *J Geophys. Res , 96*, 13,067-13,071, 1991.

Yavitt, J. B., Methane and carbon dioxide dynamics in *Typha latifolia (L.)* wetlands in central New York State, *Wetlands, 17*, 394-406, 1997.

P A. Leffelaar and R Segers, Group Plant Production Systems, Laboratory of Theoretical Production Ecology, Wageningen University, P O Box 430, 6700 AK Wageningen, Netherlands (reinoud.segers@pp.dpw wau.nl, peter.leffelaar@pp.dpw wau.nl)

C. Rappoldt, Biological Centre, University of Groningen, P O Box 14, 9750 AA Haren, Netherlands. (c.rappoldt@biol.rug.nl)

(Received August 19, 1999, revised July 13, 2000; accepted August 2, 2000.)